# Angle Spectrum Expanded Light-Field Holography Display Using Spatial-Temporal Multiplex

*Wenqi Wang, Qing He, Sen Liu, Jun Xia**

**Joint International Research Laboratory of Information Display and Visualization, Southeast University, Jiangsu, China**

## Abstract

*A light-field holographic display technology based on spatial-temporal multiplexing is proposed, which redistributes the light-field information into different spatial locations and temporal frames. This approach solves the spectrum aliasing for high resolution light-field hologram. As a result, the three-dimensional holographic display is perceived by the human eye with a continuous motion parallax with wider viewing angle, and is particularly suitable for applications such as augmented reality and virtual reality.*

## Author Keywords

Holographic display; Light field; Augmented Reality; Optical imaging.

## 1. Introduction

In recent years, light-field holography has emerged as a transformative technology that offers highly immersive and realistic three-dimensional (3D) visual experiences. By capturing and reproducing the full angular and spatial information of a scene, light-field displays enable viewers to perceive depth, motion parallax, and natural focusing, mimicking real-world viewing conditions [1–4]. This technology is crucial for applications such as augmented reality (AR), virtual reality (VR), and the metaverse, where lifelike 3D representation is essential for enhancing user interaction and presence [5–7]. However, achieving both high spatial and angular resolution in light-field holography remains a significant challenge due to the inherent limitations of space-bandwidth product and hardware constraints [8].

In our previous work, we introduced a method of encoding light-field information into a hologram using spectral expansion, which allowed for light-field displays at different viewpoints. However, due to the limitations imposed by the space-bandwidth product, this method could only compute a limited number of viewpoints, which resulted in a reduction in the angular resolution of the light field. While this approach was a significant advancement, it still faced challenges in achieving higher angular resolution and wider viewing angles, especially in real-time applications with complex 3D scenes.

To address these limitations, we propose an improved method that utilizes spatial-temporal multiplexing to expand the angle spectrum of light-field holography. By distributing the spatial and angular resolution information across different temporal frames, our method effectively increases the amount of information conveyed through the system. This approach significantly enhances the viewing angle and resolution by increasing the frame rate, enabling users to experience a more immersive and high-quality visual display. Moreover, the use of spatial-temporal multiplexing allows for a more efficient use of limited hardware resources, making the system viable even under hardware constraints.

This new method holds significant potential for advancing light-field holographic displays, providing a wider field of view and higher angular resolution without the need for additional hardware upgrades. As a result, this technology can enable the development of display systems with greater visual clarity and stability, contributing to a more realistic and immersive 3D viewing experience.

## 2. Method and results

Figure 1 illustrates the schematic diagram of a spatial-temporal multiplexed light-field holographic display. The method realizes the convergence of plane waves at different depths by assigning different orientation information of a 3D object to different temporal frames. With this technique, the observer is able to perceive the continuous motion parallax of the light field within the visual range and experience a natural depth-of-field effect. In the schematic, a 3D model of a cat is divided into four depth planes as an exemplary demonstration of the variation of different depth levels. The human eye, within the viewing range (eye box), can see different angles of the cat model and adjust the focus to observe the details on the different depth planes, thus presenting a richer 3D visual effect.

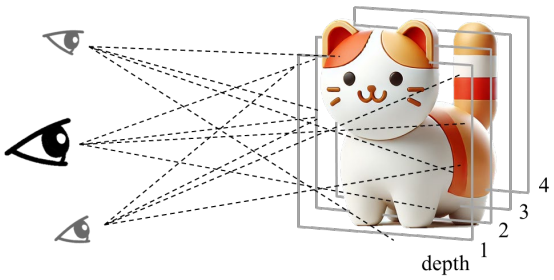


**Figure 1.** Schematic diagram of expanded spectrum light-field holographic display using spatial-temporal multiplexing

We use stochastic gradient descent to optimize the computation of holograms. A number of holograms $h_{(v_x,v_y,n)}$ are generated as shown in Equation 1:

$$h_{(v_x,v_y,n)} = f_O\left\{L_O\left\{u_{(v_x,v_y,n)}, u_{t(v_x,v_y,n)}\right\}\right\}, (v_x = 1, \dots i, v_y = 1, \dots j, n = 1, \dots N) \quad (1)$$

where $u_{(v_x,v_y,n)}, u_{t(v_x,v_y,n)}$ denote the reconstructed complex amplitude and target complex amplitude at each time step $N$, respectively. $L_O$ denotes the loss function, $f_O$ denotes the optimization system, $v_x, v_y$ denote the angular resolution of the light field in transverse and longitudinal coordinates, respectively. $i, j$ denote the ordinal number of the light field in transverse and longitudinal coordinates, respectively.

To reconstruct the complex amplitude, we use a simple Fourier transform for the calculation. As shown in Equations 2–3. In the previous calculation process [9–10], we encode the light field information into a hologram for light field display by the method


ISSN 0097-996X/25/5602-0704-$1.00 © 2025

of expanded spectrum. However, this calculation method can only calculate fewer viewpoints in order to ensure the imaging quality due to the limitation of the spatial bandwidth product, which leads to insufficiently high angular resolution of the light field. Therefore, we solve this problem by spatial-temporal multiplexing.

$$u_{(v_x,v_y,n)} = \mathcal{F}^{-1}\left\{\mathcal{F}\left\{u_{s(v_x,v_y,n)}\right\} \cdot W_{(v_x,v_y,n)}\right\}(v_x = 1, \dots i, v_y = 1, \dots j, n = 1, \dots N) \quad (2)$$

$$W_{(v_x,v_y,n)} = \begin{cases} 1, f_x^2 + f_y^2 \le 1 \\ 0, f_x^2 + f_y^2 > 1 \end{cases} \quad (3)$$

where $W_{(v_x,v_y,n)}$ denotes the spectral filter and $\mathcal{F}, \mathcal{F}^{-1}$ denotes the Fourier transform and its inverse transform, respectively, and $f_x, f_y$ denotes the horizontal and vertical coordinates of the spectrum respectively.

In addition, the center point of the filter will be shifted with the unused spectral positions corresponding to plane waves at different angles of the light field.

The specific flow is given in Figure 2. We optimize each time step separately to obtain a series of holograms. Finally, they are loaded on the spatial light modulator in chronological order to complete the display. Specifically, we take a random phase as the input to the system, and obtain the spectral information by fast Fourier transform. At this point, the corresponding spectral filter $W_{(v_x,v_y,n)}$ is used to filter out the high-frequency noise. Then the Fourier inverse transform is performed again to calculate the loss function between the output reconstructed complex amplitude and the target complex amplitude, and the gradient calculation is performed using the Adam optimizer to iteratively update the input phase, and the optimized hologram is finally obtained. Among them, the target complex amplitude consists of a predefined tilt phase together with the target amplitude, aiming to simulate the phase shifts of the plane waves of the light field in different angular directions to obtain an array of displacement points in the spectral plane, which together form the visual range of the human eye.

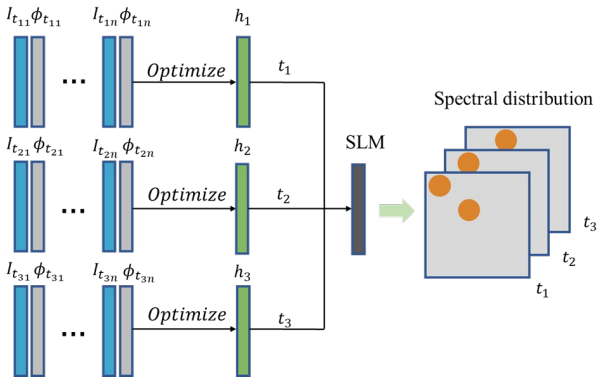


**Figure 2.** Flowchart for optimizing the computation of light-field holograms

We evaluated the obtained results using the peak signal-to-noise ratio (PSNR) and the structural similarity index (SSIM), the values of which are shown in Table 1. For 9 × 9 light field images, there are 81 corresponding quality parameters. In this paper, we show only the first 9 sets of parameters as a demonstration. The SSIM value of the image reconstruction basically reaches above 0.99, and the PSNR value exceeds 40, indicating that the reconstruction effect is excellent and the quality is more satisfactory.

We have carried out simulation validation by the proposed method, calculated the light fields of 3 × 3 and 9 × 9 viewpoints, and successfully obtained high-quality reconstructed images. Among them, the simulation results for the 9 × 9 viewpoint are shown in Figure 3. Due to space limitation, we only show thumbnails of the reconstruction results, with the first image boxed in red and placed in the lower right corner for highlighting and zooming in.

**Table 1.** PSNR and SSIM evaluated values of 9×9 light field images reconstruction results

| | SSIM | PSNR |
|---|---|---|
| *Image1* | 0.9902 | 44.42 |
| *Image2* | 0.9909 | 44.81 |
| *Image3* | 0.9915 | 45.09 |
| *Image4* | 0.9916 | 45.17 |
| *Image5* | 0.9916 | 45.09 |
| *Image6* | 0.9916 | 45.15 |
| *Image7* | 0.9915 | 45.18 |
| *Image8* | 0.9913 | 45.43 |
| *Image9* | 0.9912 | 44.85 |

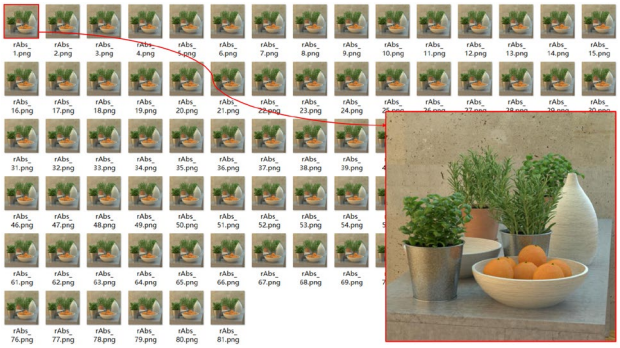

**Figure 3.** Optical field holographic display simulation reconstruction results

Next, we built an experimental light path to verify the above simulation results. The schematic diagram of the experimental light path is shown in Figure 4.

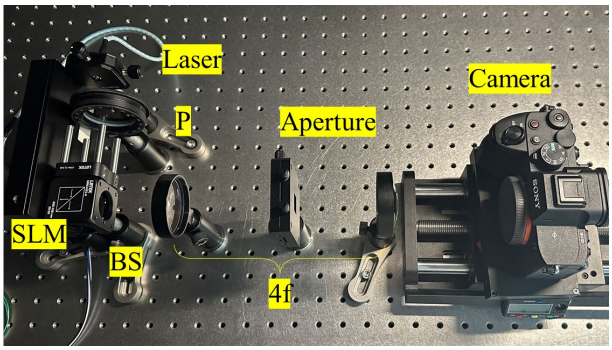


**Figure 4.** Schematic diagram of the physical setup. P, polarization. BS, beam splitter

In the figure, a beam of coherent light is emitted from a laser, passes through a polarizer to adjust its polarization state, is collimated by a lens, and then irradiated onto the surface of a spatial light modulator to achieve phase modulation. The modulated beam enters the 4f system via a beam splitter for spatial filtering. Finally, the optically reconstructed image is recorded by the camera.

We used a SMARTVISION Xinguang-I-101 spatial light modulator for the experiments, which has a resolution of 1920 × 1080 and a pixel size of 6 μm. In addition, a Sony ILCE-7M4 camera with a resolution of 7008 × 3944 was used in the experiments to provide high-quality image capture. With this configuration, we completed the optical experiments and demonstrated the experimental results for a 3 × 3 point-of-view, as shown in Figure 5. The experimental results show that the optical field exhibits different clear surfaces at different depth locations, reflecting the depth-aware nature of the optical field reconstruction. These experiments verify the effectiveness and superiority of our method in practical applications.

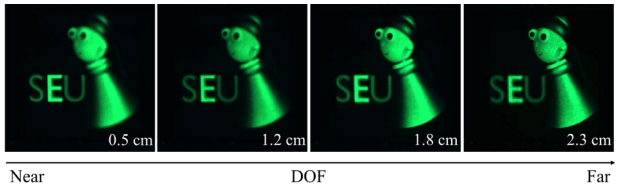


**Figure 5.** Experimental results of 3 × 3 point-of-view light field holographic reconstruction demonstrating different depth-of-field effects from near to far.

## 3. Conclusions

In this work, we demonstrate a new approach to enhance light-field holographic displays by employing a spatial-temporal multiplexing technique where we combine the angular information of the light field with different temporal frames, thereby increasing the amount of spatial and angular information that can be captured and displayed. This technique reduces the spectral aliasing of high-resolution light-field holograms and greatly improves the quality of light-field holograms, providing a richer visual experience. The introduction of this approach lays the foundation for the future development of holographic display technology for AR and other immersive technologies.

## 4. Acknowledgements

National Key R&D Program of China (grant No. 2021YFB3600502); National Natural Science Foundation of China (grant No. 62075040)

## 5. References

1. Yamaguchi M. Light-field and holographic three-dimensional displays [Invited]. J. Opt. Soc. Am. A, 2016, 33(12), 2348-2364.
2. Wang D, Li N, Li Y, Zheng Y, Nie Z, Li Z, et al. Large viewing angle holographic 3D display system based on maximum diffraction modulation. Light Sci. Appl. 2023, 4,18.
3. Schiffers F, Chakravarthula P, Matsuda N, Kuo G, Tseng E and Lanman D. Stochastic Light Field Holography, 2023 IEEE International Conference on Computational Photography (ICCP), Madison, WI, USA, 2023, 1-12
4. Peng Y, Choi S, Padmanaban N and Wetzstein G. Neural holography with camera-in-the-loop training. ACM Trans. Graph. 2020, 39, 185.
5. Xiong J, Hsiang E, He Z, Zhan T, and Wu S. Augmented reality and virtual reality displays: emerging technologies and future perspectives. Light Sci Appl. 2021, 10, 216.
6. Choi S, Gopakumar M, Peng Y, Kim J, and Wetzstein G. Neural 3D holography: learning accurate wave propagation models for 3D holographic virtual and augmented reality displays. ACM Trans. Graph. 2021, 40, 6, 240.
7. Chang C, Bang K, Wetzstein G, Lee B, Cao L. Toward the next-generation VR/AR optics: a review of holographic near-eye displays from a human-centric perspective. Optica, 2020, 7(11), 1563.
8. Padmanaban N, Peng Y, and Wetzstein G. Holographic near-eye displays based on overlap-add stereograms. ACM Trans. Graph. 2019, 38(6), 214.
9. Wang W, Xia J, Liu S, Cai Y and Chen Y. Complex Holographic Display via Spatial Complex Light Modulation. Proceedings of the International Display Workshops (IDW), Niigata, Japan, 2023, PRJ4.
10. Wang W, Liu S, Zhang Z, et al. Large screen size transparent display using spectrum expanded light field holograms. Optics Express, 2025, 33(2/27), 1883–1897.